

# Proton structure from electron-proton deep inelastic scattering

William L. Stubbs  
ift22c@bellsouth.net

**Abstract:** The proton  $F_2$  structure function curve reveals the number and type of particles inside the proton. Deep inelastic scattering experiments from the late 1960s produced an  $F_2$  curve with no data for proton momentum fractions less than 0.06. However, the assumption the missing  $F_2$  values remain constant in that region provided the basis for the current proton model of quarks and gluons. Here, I produce a complete proton  $F_2$  curve by combining data generated in 2000 with the original 1960s data. It shows the aforementioned assumption was wrong, invalidating the basis for the quark-gluon proton. My analysis of the new curve indicates protons are made of nine particles that appear to be muons; each of which is made of approximately 204 particles that look like electrons.

The current proton model evolved out of deep inelastic scattering experiments done at the Stanford Linear Accelerator Center (SLAC) in the late 1960s (1, 2). Electron-proton ( $e-p$ ) deep inelastic scattering shoots high-energy (GeV) electrons into protons, where they scatter off the particles inside. The cross sections, angles and energies of the scattered electrons are measured and used along with the initial electron energies to produce information about those particles (3). SLAC did the first of these experiments in 1967, measuring the cross sections of scattered electrons with initial energies between 4.6 GeV and 20 GeV, and scattering angles from  $6^\circ$  to  $34^\circ$  (4, 5). From those experiments, they discovered charged (6), spin  $\frac{1}{2}$  (7) particles inside the proton. After that, the perceived design of the proton became strongly influenced by SU(3) theory proposed by Gell-Mann (8) and Zweig (9) in 1964. It modeled the proton as three charged, spin  $\frac{1}{2}$  particles Zweig called aces and Gell-Mann called quarks, the name that stuck.

By 1969, SLAC had produced an  $F_2$  structure function curve for the proton (3). The proton  $F_2$  structure function values are quantities that characterize the momentum distribution of the particles inside the proton (10). Each particle within the proton carries a fraction  $x$  of the proton's momentum. The  $F_2$  value relates to the probability a particle inside the proton has proton momentum fraction  $x$  (3). For the proton to be made of just three quarks, the  $F_2$  values must go to zero as  $x$  goes to zero (11) and the  $F_2$  curve should peak at  $x \approx \frac{1}{3}$  (3). Figure 1A is the SLAC curve, which plotted the  $F_2$  values as a function of  $x$ . The figure shows the curve had no data for  $0 \leq x < 0.06$ . However, although the  $F_2$  curve was incomplete, it did not appear to support Gell-Mann's simple 3-quark model of the proton (11), and the model was dismissed. Nonetheless, finding a way to incorporate the quarks into the proton model became a primary focus of the SLAC modeling effort (2, 11). Consequently, as the effort progressed, interpretations of, and assumptions about, data collected biased toward validating quarks.

An assumption that the  $F_2$  values remain constant as  $x \rightarrow 0$  was drawn from the incomplete proton  $F_2$  curve. It became the basis for the final proton model consisting of three valence quarks and undetermined numbers sea quarks and gluons (11, 12), which was in place by the early 1970s (13). Deep inelastic scattering experiments done at the Hadron Electron Ring Accelerator (HERA) in the 1990s appeared to fill in the  $F_2$  curve gap left by SLAC (14). Figure 1B shows the HERA  $F_2$  values plotted on the SLAC curve in Fig. 1A. The HERA  $F_2$  values rise as  $x \rightarrow 0$ , considered further evidence of sea quarks and gluons in the proton (15). They appear to validate that the  $F_2$  values do not go to zero as  $x \rightarrow 0$ . However, the momentum transfers,  $Q^2$ , in HERA were much higher than in SLAC. The higher energies used to generate the higher  $Q^2$  values in HERA produced electrons with much shorter wavelengths than in SLAC. Shorter electron wavelengths see finer detail. As a result, electrons in HERA could project a much

higher resolution of the inside of the proton than those in SLAC. This made the two sets of data incompatible and the  $F_2$  curve invalid.

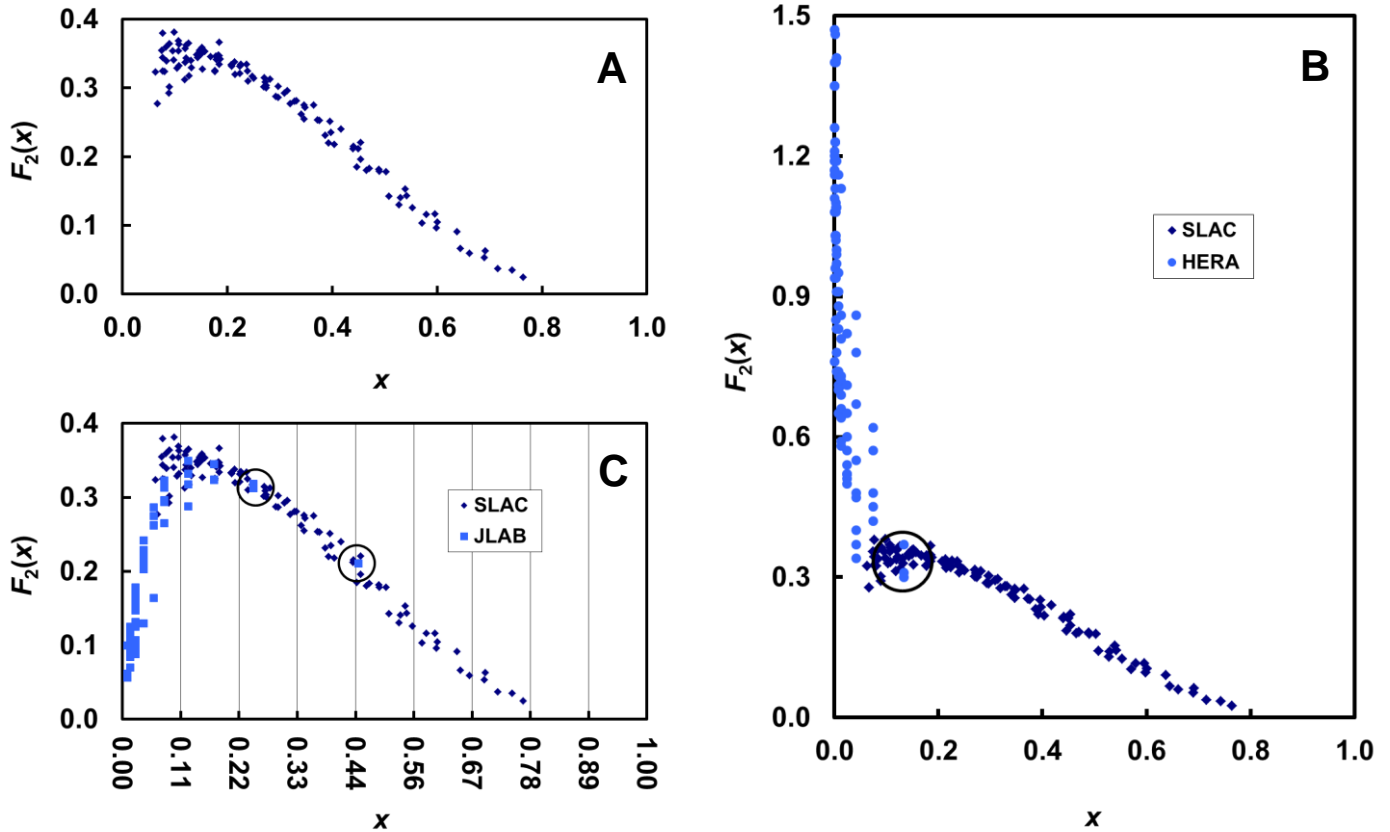


**Fig. 1: Proton  $F_2$  Structure Function Curves.** (A) The SLAC proton  $F_2$  structure function values plotted as a fraction of the proton momentum fraction  $x$  (SLAC data tabulated in Table S1). (B) Proton  $F_2$  values from HERA deep inelastic scattering overlaid on graph of SLAC  $F_2$  values (HERA data tabulated in Table S2). The circle shows HERA points among SLAC data. (C) The SLAC proton  $F_2$  structure function curve with JLAB  $F_2$  values at low- $x$  appended (JLAB data tabulated in Table S4). The circled JLAB points show how well they integrate into the SLAC data. The  $x$ -axis is graduated in ninths to show the  $F_2$  values peaks at  $x = 1/9$ .

Here I produce a truly complete proton  $F_2$  curve by combining the 1960s SLAC  $F_2$  values with values from deep inelastic scattering done in 2000 at similar momentum transfers. I use that curve to determine the structure inside the proton consistent with the experimental data. I then reanalyzed the HERA data, in light of the newly determined proton structure, and then modify that structure to incorporate the HERA findings.

I created the complete proton  $F_2$  structure function curve using data generated at the Thomas Jefferson National Accelerator Facility (JLAB). In 2000, it did a series of  $e-p$  deep inelastic scattering experiments (16) at momentum fractions from  $x = 0.009$  to  $x = 0.45$ . This range included most of the  $x < 0.06$  region not covered by the SLAC experiments. These experiments used electron energies comparable to those used in the SLAC experiments from the late 1960s. The electron-proton momentum transfers in the JLAB experiments span from  $Q^2 = 0.034 \text{ GeV}^2$  up to  $Q^2 = 2.275 \text{ GeV}^2$ , with  $Q^2 < 1.0 \text{ GeV}^2$  for all experiments with  $x < 0.1$ . Most of the

scatterings done at SLAC with  $x < 0.17$  were at momentum transfers of  $Q^2 < 2.0 \text{ GeV}^2$  and many at  $Q^2 < 1.0 \text{ GeV}^2$ . As a result, the JLAB electrons saw inside the proton at the same resolution as the electrons from the SLAC experiments. This makes the JLAB  $F_2$  values a true extension of the SLAC data at low proton momentum fractions. In Fig. 1C, I plotted the JLAB proton  $F_2$  values onto the curve with the SLAC values from Fig. 1A. This produced the complete  $F_2$  structure function curve for the proton.

Figure 1C shows that as  $x \rightarrow 0$ , the  $F_2$  values also go to zero, with the  $F_2$  curve peaking at about  $x = 1/9$ . The figure also shows the  $F_2$  values of the two data sets compare well at common momentum fractions. For momentum fractions from  $x = 0.06$  to  $x = 0.2$ , the JLAB  $F_2$  values are literally on top of the SLAC values. This means that in this region JLAB and SLAC were seeing the same things inside the proton. As further validation of their compatibility, I circled the three JLAB  $F_2$  values that fell on the slope of the curve beyond  $x = 0.2$ , to show how well they integrate into the SLAC data. The two JLAB  $F_2$  values at  $x = 0.25$  and the one at  $x = 0.45$  are literally engulfed by the SLAC data.

Feynman called the particles found inside the proton, partons (13, 17). He assumed the  $e-p$  inelastic scattering occurs in the infinite momentum frame of reference, where the proton is moving near light speed while the electron is standing still (18). Then, time dilation slows down the motion of the partons inside the protons, so that an impulse approximation (19) may be applied to high-energy collisions. There, incident electrons scatter incoherently off individual partons that are instantaneously free from the other partons in the proton. Bjorken and Paschos expanded upon the parton model (11), determining that the  $F_2$  values for a proton made of a finite number of partons should go to zero as  $x \rightarrow 0$ .

Figure 2 shows the SLAC proton  $F_2$  data Bjorken had, plotted as a function of  $\omega$ , a graph similar to the one he used. Here,  $\omega = 1/(2Mx)$ , where  $M$  is the proton mass,  $0.938 \text{ GeV}$  (11). Since  $\omega$  is a scalar multiple of  $1/x$ , for the three-quark proton model to be valid,  $F_2$  must now go to zero as  $\omega \rightarrow \infty$ . From about  $\omega = 3.0 \text{ GeV}^{-1}$ , as  $\omega$  increases, the  $F_2$  values appear to stay constant. They do not appear headed toward zero as  $\omega \rightarrow \infty$ . Therefore, Bjorken and Paschos ruled out a proton made of a finite number of particles, including the simple three-quark proton (11). Figure 1A shows the same  $F_2$  data plotted in Fig. 2 as a function of  $x$ . Again, it does not appear  $F_2 \rightarrow 0$  as  $x \rightarrow 0$ , the condition now required. However, Fig. 1A shows there was no data for  $x < 0.06$ .

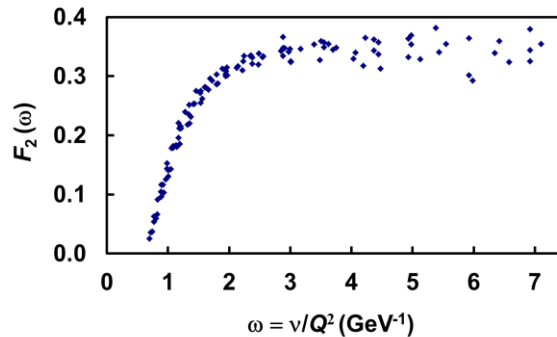


**Fig. 2: Proton  $F_2$  Structure Function Curve.** The SLAC proton  $F_2$  structure function values plotted as a function of  $\omega = 1/(2Mx)$ . The above graph shows variable  $\omega = \nu/Q^2$  to be consistent with the plot in Fig. 2 of Ref. 11. However,  $\nu/Q^2 = 1/(2Mx)$ .

The  $F_2$  data appearing to remain constant for  $\omega > 3$  in Fig. 2 led Bjorken and Paschos to assume the proton  $F_2$  remained constant as  $x \rightarrow 0$  (11). Based on this, they developed a case for a proton made of the three quarks, now called “valence” quarks, immersed in a background of quark-antiquark pairs they called a pion cloud, which we call “sea” quarks, today (11). The JLAB data shows that the Bjorken and Paschos assumption was wrong. Consequently, their justification for the existence of sea quarks in the proton appears to be invalid.

According to the parton theory, the  $F_2$  curve peaks at the momentum fraction equal to the reciprocal of the number of particles in the target (3, 20). My complete proton  $F_2$  curve peaking at  $x = 1/9$  indicates the proton is made of nine particles. That means the particles inside the proton have a mass of  $1/9$  the proton’s mass. I surveyed the subatomic particles (21) and found that the mass of the muon is about  $1/9$  that of the proton. The muon is also a spin  $1/2$ , charged particle, the other attributes of the particles inside the proton revealed by the  $e-p$  deep inelastic scattering. Therefore, muons are the particles likely forming the proton. To get the proton’s +1 charge, it must be made of four muons and five antimuons.

The mass of a free proton is 938.27 MeV. This makes the mass of each of its nine partons 104.25 MeV, which is just 1.41 MeV less than the 105.66 MeV mass of the free muon. I recognized the reduced muon mass inside the proton resembles that observed of nucleons within the nucleus. There, the nucleons interact with each other through a binding mechanism that holds the nucleus together and creates the mass defect. If the nine muons that make up the proton bind to each other in a similar way, they likely experience a similar mass defect within the proton. As a result, the muons inside the proton are slightly less massive than a free muon. Nine free muons have a mass of 950.94 MeV, 12.67 MeV more than the proton’s mass of 938.27 MeV. Therefore, it appears the mass defect and binding energy of the proton is 12.67 MeV.

Muons binding to each other to form the proton also aligns with another tenant of parton theory; that the  $F_2$  values distribute over the whole range of proton  $x$  values because the partons interact with each other (3, 20). If the partons did not interact inside the proton, the proton  $F_2$  would equal 1 at  $x$  equal to the reciprocal of the number of particles in the proton, and 0 for all other values of  $x$  (3, 20). Since the  $F_2$  values distribute over  $x$ , the partons inside the proton apparently interact with each other.

Combining the SLAC and JLAB  $F_2$  data showed that the proton is made of nine particles, apparently muons, eliminating the bases for sea quarks and gluons in the proton thought shown by the HERA data. That means the HERA data is revealing something else about the inside of the proton. I noticed that at momentum fraction  $x = 0.133$ , the proton  $F_2$  values from the HERA data average 0.327 (14), while for  $x = 0.125$ , the JLAB proton  $F_2$  values average 0.322 (16). Both averages fall within the scattering of  $F_2$  values plotted on the SLAC proton  $F_2$  curve in the vicinity of  $x = 0.13$  (see Fig. 1A). This means all three experiments saw the same thing inside the proton at this momentum fraction. However, as  $x \rightarrow 0$ , the  $F_2$  values from the HERA and JLAB experiments diverge. At roughly  $x = 0.08$ , the HERA  $F_2$  value had climbed to about 0.5 compared to  $F_2 \approx 0.3$  for JLAB. Because the HERA  $F_2$  values were rising, I wondered if its electrons had begun probing a target different from the proton. With its higher resolution, I suspected HERA had transitioned from just seeing inside the proton, to seeing inside the muons inside the proton.

To test my hypothesis, I needed a muon  $F_2$  curve. HERA calculated the  $F_2$  values it reported relative to the proton. They are proton  $F_2$  values. To convert them to muon  $F_2$  values, I first had to express them in terms of muon momentum fractions. Since each muon carries  $1/9$  the proton’s momentum, the fraction of a muon’s momentum a particle carries is nine times the fraction of a

proton's momentum it carries. Therefore, I simply multiplied an  $F_2$ 's proton momentum fraction by nine to make it a muon momentum fraction. For example, an  $F_2$  value for a proton  $x$  of 0.075 has an  $x$  value of 0.675 for the muon. The muon momentum fraction cannot be greater than one, so I did not use any  $F_2$  values for proton momentum fractions greater than  $1/9$ .

Next, I adjusted the proton  $F_2$  values to represent the muon. I realized that on the proton  $F_2$  graph,  $x = 1/9$  for the proton is  $x = 1$  for the muon. This is where I assumed the HERA electrons transition to probing the muon. At  $x = 1$  on an  $F_2$  plot,  $F_2 = 0$ . So, the muon  $F_2$  value at  $x = 1/9$  on the proton graph should be zero on the muon graph. To make this happen, I subtracted the proton  $F_2$  value at  $x = 1/9$  from all of the proton  $F_2$  values for  $x \leq 1/9$ , to convert them to muon  $F_2$  values. To get a proton  $F_2$  value for  $x = 1/9$ , I calculated the average of all the measured  $F_2$  values for  $x = 1/9 \pm 0.005$  (22), which was  $F_2 = 0.352$ . With that, to convert the HERA proton  $F_2$  values for  $x \leq 1/9$  to muon values, I just subtracted 0.352 from them.

Table 1 shows the HERA proton  $F_2$  values from 1993 (14) that I averaged over  $Q^2$  in column 2 for the given proton momentum fractions in column 1. It also shows the muon  $F_2$  values I adjusted from proton values in column 4, with the corresponding muon momentum fractions I converted from proton values in column 3. The muon  $x$  values are just the proton  $x$  values multiplied by 9, and the muon  $F_2$  values are just the proton  $F_2$  values, less 0.352.

**Table 1:** The proton  $F_2$  structure function data from the 1993 HERA proton deep inelastic scattering experiments averaged for momentum fraction  $x$  (from data tabulated in Table S2); and those values converted to muon  $x$  (proton  $x$  times 9) and  $F_2$  (proton  $F_2 - 0.352$ ) values.

Proton Data		Muon Data	
$x$	$F_2$	$x$	$F_2$
0.000178	1.187	0.001602	0.835
0.000261	1.275	0.002349	0.923
0.000562	1.353	0.005058	1.001
0.000825	1.320	0.007425	0.968
0.001330	1.173	0.011970	0.821
0.002370	1.123	0.021330	0.771
0.004210	0.991	0.037890	0.639
0.007500	0.815	0.067500	0.463
0.013300	0.736	0.119700	0.384
0.023700	0.594	0.213300	0.242
0.042100	0.565	0.378900	0.213
0.075000	0.508	0.675000	0.156

I plotted the muon  $F_2$  data from Table 1 in Fig. 3A. The resulting curve has the characteristics of inelastic electron scattering in a larger particle made of a finite number of smaller particles described by Bjorken (11). The  $F_2$  values start out at near zero for  $x = 1$ . Then as  $x$  moves toward zero, the  $F_2$  values rise until they reach a peak, after which as  $x \rightarrow 0$  from the peak,  $F_2 \rightarrow 0$ . I recognized this as the  $F_2$  curve of electrons scattering off a finite number of particles inside the muons that formed the proton. I plotted the portion of the  $F_2$  curve in Fig. 3A from  $x = 0$  to  $x = 0.1$  that contains the peak  $F_2$  value in Fig. 3B. To analyze the muon  $F_2$  data, I was able to fit it with two curves. One for the three rising  $F_2$  values that fall between  $x = 0$  and  $x = 0.005058$ , the momentum fraction of the highest  $F_2$  value measured; and another for the 10 falling  $F_2$  values from  $x = 0.005058$  to  $x = 1$ . I fit the rising portion of the muon  $F_2$  curve with the natural logarithm equation

$$F_2(x) = 0.1388 \ln(x) + 1.7423,$$

and I fit the falling  $F_2$  values with natural logarithm equation

$$F_2(x) = -0.1866 \ln(x) + 0.0160.$$

Due to their slopes, I assumed the peak muon  $F_2$  occurs at the momentum fraction where the two curves intersect, which is  $x = 0.004966$ . The reciprocal of this momentum fraction indicates a muon contains in the neighborhood of 202 particles. I knew the mass of a free muon is equal to about 207 electron masses, and from the SLAC/JLAB  $F_2$  analysis, that the average mass of the muons in the proton, 104.25 MeV, is equivalent to about 204 electron masses. Since the particles inside the muon are still charged particles with spin  $\frac{1}{2}$ , I concluded the particles HERA saw inside the muon were electrons.

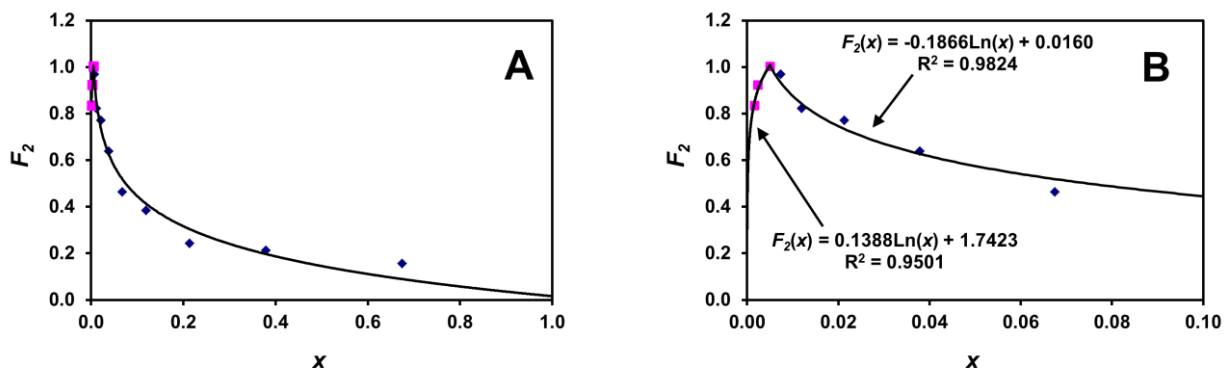


**Fig. 3: Muon  $F_2$  Structure Function Curves.** (A) The HERA muon  $F_2$  structure function values (Table 1) plotted as a function of the fraction of muon momentum,  $x$ . (B) Graph A for momentum fractions,  $x = 0$  through  $x = 0.1$  with curve fits for rising and falling segments.

My HERA analysis results suggest that the free muon is made of 207 electrons and the muons inside the proton, 204. Because the muon is a charged particle, it must be made of a combination of electrons and positrons. To have a charge of -1, free muons must contain 103 positrons and 104 electrons. Antimuons must be made of 104 positrons and 103 electrons. I noticed the muon  $F_2$  peak is sharp and at a value in the neighborhood of  $F_2 = 1$ . This indicates the electrons and positrons inside the muon do not interact strongly with each other (3, 20). I suspect the interaction is probably not binding, but electrostatic interaction due to their charges.

Assuming the muons and antimuons inside the proton are made of electrons and positrons; then the proton is also ultimately made of electrons and positrons. With a mass of just over 1,836 electron masses, it appears the proton must be made of 1,837 electrons and positrons, since it needs an odd number to have a net charge. To have a charge of +1 containing 1,837 electrons and positrons, the proton must be made of 919 positrons and 918 electrons.

A proton made of muons and electrons has the potential to address a number of observations and issues. A proton made of muons instead of quarks explains why no quarks appear after protons are shattered in high-energy collisions (21), but muons and antimuons routinely appear (19, 23). A proton made of electrons and positrons provides a source for the particles expelled from the nucleus during beta decay, missing since neutrons replaced electrons in the nucleus in

1932 (24). A proton made of muons and electrons also calls into question the validity of quantum chromodynamics (QCD), which was, in part, formulated to support the existence (or seeming nonexistence) of quarks and gluons (25). Finally, assume the neutron is a minor modification of the proton, likely 2 electrons and 1 positron, making it 920 electrons and 920 positrons. Then, protons (and neutrons) made of electrons and positrons appear to show that there is little, if any, matter-antimatter imbalance in the universe (26). In a neutral atom, there then would be 919 positrons, 918 electrons and an orbital electron for each proton, and 920 positrons and 920 electrons for each neutron. Therefore, in every neutral atom there would be a positron (antimatter) for every electron (matter).

## References

1. M. Riordan, The discovery of quarks. *Science* **256**, 1287, (1992).
2. A. Bodek, The structure of the nucleon, three decades of investigation (1967-2004). *Nucl. Phys. B – Proc. Suppl.* **139**, 165 (2005).
3. B. Povh, *et al.*, “Deep inelastic scattering” in *Particles and Nuclei: An introductory to the physical concepts*, (Springer, Berlin, ed. 8, 2008), Chap. 7 (Translated by Martin Lavelle).
4. E.D. Bloom, *et al.*, High-energy inelastic  $e-p$  scattering at  $6^\circ$  and  $10^\circ$ . *Phys. Rev. Lett.* **23**, 930 (1969).
5. G. Miller, *et al.*, Inelastic electron-proton scattering at large momentum transfers and the inelastic structure functions of the proton. *Phys. Rev. D* **5** 528 (1972).
6. J.D. Bjorken, Asymptotic sum rules at infinite momentum. *Phys. Rev.* **179** (1969) 1547.
7. C.G. Callan, D.J. Gross, High-energy electroproduction and the constitution of the electric current. *Phys. Rev. Lett.* **22** 156 (1969).
8. M. Gell-Mann, A schematic model of baryons and mesons. *Phys. Lett.* **8** 214 (1964).
9. G. Zweig, An SU(3) model for strong interaction symmetry and its breaking II, (Tech. Rep. CERN-8419-TH-412, CERN, 1964).
10. A. Bodek, *et al.*, Experimental studies of the neutron and proton electromagnetic structure functions. *Phys Rev D* **20**, 1471 (1973).
11. J.D. Bjorken, E.A. Paschos, Inelastic electron-proton and  $\gamma$ -proton scattering and the structure of the nucleon. *Phys. Rev.* **185**, 1975 (1969).
12. J. Kuti, V.F. Weisskopf, Inelastic lepton-nucleon scattering and lepton pair production in the relativistic quark-parton model. *Phys. Rev. D* **4**, 3418 (1971).
13. R.P. Feynman, Structure of the proton. *Science* **183**, 601 (1974).
14. T. Ahmed, *et al.* (H1 Collaboration), A measurement of the proton structure function  $F_2(x, Q^2)$ . *Nucl. Phys. B*, **439**, 471 (1995).
15. C. Adloff, *et al.* (H1 Collaboration), On the rise of the proton structure function  $F_2$  towards low  $x$ . *Phys. Lett. B* **520**, 183 (2001).

16. V. Tvaskis, *et al.*, Proton and deuteron  $F_2$  structure function at low  $Q^2$ . *Phys. Rev. C* **81**, 055207, 305 (2010).
17. R.P. Feynman, Very high-energy collisions of hadrons. *Phys. Rev. Lett.* **23**, 1415 (1969).
18. S.D. Drell, *et al.*, Theory of deep-inelastic lepton-nucleon scattering and lepton pair annihilation processes. II. Deep inelastic electron scattering. *Phys. Rev. D* **1** 1035 (1970).
19. S.D. Drell, T.M. Yan, Massive lepton-pair production in hadron-hadron collisions at high energies. *Phys. Rev. Lett.* **25**, 316 (1970).
20. F. Halzen, A.D. Martin, “Partons” in *Quarks & Leptons: An introductory course in modern particle physics*, (Wiley, New York, 1984), Chap. 9.
21. J. Beringer *et al.*, Review of particle physics. *Phys. Rev. D* **86**, 010001, 30 (2012).
22. L.W. Whitlow, “Deep inelastic structure functions from electron scattering on hydrogen, deuterium, and iron at  $0.6 \text{ GeV}^2 \leq Q^2 \leq 30.0 \text{ GeV}^2$  (Appendix E)” (Tech. Rep. SLAC- 357, SLAC, 1990).
23. A. Aktas, *et al.* (H1 Collaboration), Muon pair production in ep collisions at HERA. *Phys. Lett. B*, **583**, 28 (2004).
24. F.L. Wilson, Fermi’s theory of beta decay. *Am. J. Phys.* **36**, 1150 (1968).
25. P.Z. Skands, <http://arxiv.org/abs/1207.2389> (2015).
26. H.R. Quinn, “The symmetry, or lack of it, between matter and antimatter” (Tech. Rep. SLAC-PUB-8784, SLAC, 2001).

## Supplementary Materials

Materials and Methods  
Tables S1 and S4

## Supplementary Materials

### Materials and Methods:

#### SLAC proton structure function data

The proton  $F_2$  structure function data for Figures 1A and 2 comes from Appendix E of Ref. 22 and are available at [https://www.slac.stanford.edu/exp/e140/F2.H2\\_357](https://www.slac.stanford.edu/exp/e140/F2.H2_357). I used the 117 data points labeled “1” in column “J” from the E49 experiments at  $\theta = 6^\circ$  and  $\theta = 10^\circ$ . The initial energies,  $E_0$ , scattered energies,  $E'$ , and scattering angles,  $\theta$ , of the electrons that correspond to the  $F_2$  data used are in [https://www.slac.stanford.edu/exp/e140/SIGMA.H2\\_357](https://www.slac.stanford.edu/exp/e140/SIGMA.H2_357). The file [https://www.slac.stanford.edu/exp/e140/HELP.DOC\\_357](https://www.slac.stanford.edu/exp/e140/HELP.DOC_357) discusses the formats of the aforementioned datasets. There were other experiments done at the time Bjorken and Paschos wrote their paper; however, I could not confirm SLAC processed the data in time for it to be included in their analysis. Therefore, I did not include them in the data for the figures. I listed the  $F_2$  values I used in Table S1.

#### HERA proton and muon structure function data

I got the proton  $F_2$  structure function data for Figure 1B from Ref. 14. They are listed in Table S2. The table shows the  $F_2$  values and the  $Q^2$  values for each value of  $x$ . To get the values in the column on the end labeled “Avg.”, I simply did an arithmetic average of the  $F_2$  values in that row. I used these values in Table 1 of the report. I omitted two of the  $F_2$  values from Table 1, the one for  $x = 0.000383$  and the one for  $x = 0.133$ . I saw that the  $F_2$  values from  $x = 0.000178$  up to  $x = 0.000562$  were increasing as  $x$  increased except the  $F_2$  for  $x = 0.000383$ . After the value before it had risen to 1.275, it fell back to 1.257, counter to the trend of the data. This made the value look suspicious, so I decided to leave it out. I omitted the  $x = 0.133$  value because 0.133 is greater than  $1/9$ , the maximum proton momentum fraction a muon can carry.

To get the datum proton  $F_2$  value for  $x = 1/9$  with which to adjust the HERA proton values to muon values, I calculated the average of all the measured proton  $F_2$  values from the SLAC data for  $x = 1/9 \pm 0.005$ . The values I used are in Table S3. The choice of 0.005 as the neighborhood about  $x = 1/9$  to do the averaging was somewhat arbitrary. I tried to balance making the interval small enough so that it gave a good representation of  $F_2$  at the point  $x = 1/9$ , with getting a reasonable amount of points to average. I simply added up the nine  $F_2$  values and divided the sum by nine. The result was 0.3518, which I rounded to 0.352.

I did the curve fits in Figures 3A and 3B using the “Add Trendline” option in the “Chart” tab available once a chart is inserted and the data points are plotted in Excel 2003. I used the “Logarithmic” Trend/Regression Type from the “Type” tab and selected the “Display equation on chart” and “Display R-squared value on chart” from the “Options” tab of Add Trendline.

#### JLAB proton structure function data

The proton  $F_2$  structure function data for Figure 1C comes from Ref. 16. They are listed in Table S4. The table shows the  $F_2$  values and the  $Q^2$  values determined for each value of  $x$ . I used the values directly from the source.

**Table S1.**

The proton  $F_2$  structure function values as a function of  $x$  and  $Q^2$  from the initial SLAC proton deep inelastic scattering experiments at  $6^\circ$  and  $10^\circ$  (Appendix E.4 in Ref. 22).

I	$x$	$Q^2$ (GeV <sup>2</sup> )	$F_2$
1	0.274	0.9040	0.30016
2	0.224	0.8700	0.32066
3	0.177	0.8240	0.32355
4	0.153	0.7940	0.32693
5	0.119	0.7370	0.31220
6	0.090	0.6660	0.30119
7	0.067	0.5860	0.27682
8	0.417	1.6850	0.23967
9	0.365	1.6470	0.27490
10	0.315	1.6010	0.29547
11	0.271	1.5520	0.31447
12	0.209	1.4550	0.33159
13	0.168	1.3630	0.34548
14	0.132	1.2560	0.32928
15	0.104	1.1410	0.32845
16	0.081	1.0190	0.32385
17	0.503	2.3770	0.17809
18	0.450	2.3340	0.21125
19	0.396	2.2810	0.25099
20	0.347	2.2210	0.27517
21	0.282	2.1160	0.31261
22	0.226	1.9950	0.33441
23	0.185	1.8720	0.33393
24	0.150	1.7380	0.34879
25	0.122	1.5940	0.34326
26	0.098	1.4400	0.34013
27	0.077	1.2750	0.34363
28	0.063	1.1360	0.32321
29	0.596	3.5000	0.11615
30	0.542	3.4460	0.14308
31	0.490	3.3830	0.17846
32	0.441	3.3130	0.21499
33	0.372	3.1910	0.25352
34	0.309	3.0470	0.29241
35	0.239	2.8180	0.32459
36	0.183	2.5690	0.34746
37	0.152	2.3820	0.35876
38	0.126	2.1880	0.36489
39	0.107	2.0170	0.35363

I	$x$	$Q^2$ (GeV <sup>2</sup> )	$F_2$
40	0.090	1.8450	0.36392
41	0.075	1.6580	0.35448
42	0.320	1.1040	0.27664
43	0.270	1.0530	0.30144
44	0.240	1.0160	0.30967
45	0.177	0.9120	0.32512
46	0.127	0.7910	0.31725
47	0.089	0.6570	0.29204
48	0.454	1.8710	0.22037
49	0.348	1.7410	0.27128
50	0.214	1.4690	0.33795
51	0.120	1.1150	0.33700
52	0.539	2.7620	0.15260
53	0.489	2.6930	0.18149
54	0.440	2.6160	0.21158
55	0.376	2.4940	0.25243
56	0.297	2.2970	0.30233
57	0.237	2.0980	0.33396
58	0.187	1.8800	0.34220
59	0.144	1.6440	0.34421
60	0.108	1.3880	0.33206
61	0.077	1.1140	0.32474
62	0.638	4.1480	0.09100
63	0.580	4.0450	0.11591
64	0.553	3.9910	0.12534
65	0.471	3.8040	0.18311
66	0.398	3.5940	0.23489
67	0.332	3.3570	0.28093
68	0.273	3.0920	0.30827
69	0.224	2.8190	0.33113
70	0.179	2.5090	0.34092
71	0.142	2.1890	0.34797
72	0.108	1.8340	0.36327
73	0.084	1.5420	0.33888
74	0.692	5.1800	0.06271
75	0.601	4.9820	0.10437
76	0.530	4.7960	0.14042
77	0.454	4.5530	0.19577
78	0.387	4.2940	0.23110

I	$x$	$Q^2$ (GeV <sup>2</sup> )	$F_2$
79	0.328	4.0140	0.28058
80	0.274	3.6990	0.30358
81	0.227	3.3730	0.33368
82	0.185	3.0130	0.36625
83	0.147	2.6310	0.35421
84	0.120	2.3050	0.35712
85	0.096	1.9680	0.35394
86	0.743	6.8730	0.03517
87	0.690	6.7290	0.05328
88	0.662	6.6470	0.05917
89	0.599	6.4410	0.09594
90	0.528	6.1740	0.13006
91	0.465	5.8940	0.17991
92	0.404	5.5690	0.21761
93	0.347	5.2150	0.25488
94	0.297	4.8450	0.28623
95	0.251	4.4460	0.31369
96	0.208	4.0030	0.33321
97	0.178	3.6490	0.34573
98	0.150	3.2650	0.35661
99	0.122	2.8510	0.36177
100	0.099	2.4380	0.38122
101	0.077	2.0090	0.37937
102	0.764	8.0670	0.02465
103	0.716	7.9140	0.03698
104	0.645	7.6560	0.06626
105	0.571	7.3480	0.10294
106	0.508	7.0370	0.14264
107	0.447	6.6910	0.18475
108	0.393	6.3280	0.21957
109	0.341	5.9310	0.26182
110	0.293	5.4980	0.28716
111	0.248	5.0320	0.31681
112	0.215	4.6340	0.31944
113	0.185	4.2190	0.34692
114	0.157	3.8040	0.35328
115	0.131	3.3550	0.33947
116	0.107	2.8880	0.36865
117	0.083	2.3860	0.35900

**Table S2.**

The proton  $F_2$  structure function values as a function of  $x$  and  $Q^2$  from the HERA 1993 proton deep inelastic scattering experiments (Table 4 in Ref. 14).

$x$	$Q^2$ (GeV <sup>2</sup> )																Avg.
	4.5	6	8.5	12	15	20	25	35	50	65	80	120	200	400	800	1600	
0.000178	1.16	1.21	1.19														1.187
0.000261			1.20	1.35													1.275
0.000383			1.11	1.26	1.40												1.257
0.000562				1.19	1.35	1.52											1.353
0.000825				1.08	1.17	1.17	1.71										1.320
0.00133				0.96	1.13	1.03	1.23	1.23	1.46								1.173
0.00237				0.85	0.94	1.03	1.02	1.10	1.08	1.40	1.09	1.60					1.123
0.00421				0.74	0.78	0.83	0.91	0.97	1.00	1.09	1.19	0.99	1.41				0.991
0.00750				0.70	0.71	0.74	0.73	0.88	0.65	0.95	0.70	0.83	0.91	1.16			0.815
0.0133				0.58	0.59	0.64	0.71	0.86	0.66	0.69	0.71	0.73	0.72	0.81	1.13		0.736
0.0237						0.51	0.52	0.57	0.52	0.50	0.60	0.65	0.54	0.71	0.82		0.594
0.0421								0.55	0.40	0.48	0.47	0.34	0.37	0.78	0.67	0.86	0.565
0.075											0.45	0.48		0.42	0.57	0.62	0.508
0.133														0.31	0.30	0.37	0.327

**Table S3.**

The proton  $F_2$  structure function values from the SLAC dataset used to calculate the proton  $F_2$  value at  $x = 1/9$ . The numbers in the ‘‘I’’ column are the index values of the data points in the SLAC dataset (Appendix E.4 in Ref. 22).

I	$x$	$F_2$
178	0.106	0.36051
39	0.107	0.35363
116	0.107	0.36865
60	0.108	0.33206
72	0.108	0.36327
195	0.108	0.34363
333	0.112	0.33988
166	0.113	0.35348
177	0.116	0.35139

**Table S4.**

The proton  $F_2$  structure function values as a function of  $x$  and  $Q^2$  from the JLAB E99-118 deep inelastic scattering experiments (Table II in Ref. 16).

$x$	$Q^2$ (GeV <sup>2</sup> )	$F_2$
0.009	0.034	0.0560
0.009	0.051	0.0616
0.009	0.086	0.0997
0.015	0.059	0.0696
0.015	0.095	0.0842
0.015	0.098	0.0961
0.015	0.112	0.0876
0.015	0.127	0.1058
0.015	0.144	0.1114
0.015	0.151	0.1216
0.015	0.164	0.1253
0.015	0.172	0.1118
0.025	0.067	0.0883
0.025	0.092	0.0960
0.025	0.104	0.1040
0.025	0.113	0.1069
0.025	0.140	0.1251
0.025	0.186	0.1469
0.025	0.195	0.1312
0.025	0.212	0.1675
0.025	0.222	0.1593
0.025	0.240	0.1780
0.025	0.252	0.1696
0.025	0.253	0.1530
0.025	0.287	0.1669
0.040	0.133	0.1295
0.040	0.273	0.2038

$x$	$Q^2$ (GeV <sup>2</sup> )	$F_2$
0.040	0.287	0.2027
0.040	0.353	0.2244
0.040	0.370	0.2288
0.040	0.371	0.2186
0.040	0.380	0.2102
0.040	0.421	0.2416
0.060	0.180	0.1641
0.060	0.479	0.2622
0.060	0.491	0.2617
0.060	0.543	0.2751
0.060	0.633	0.2863
0.080	0.456	0.2650
0.080	0.617	0.2935
0.080	0.619	0.2960
0.080	0.799	0.3128
0.080	0.818	0.3227
0.125	0.588	0.2876
0.125	0.797	0.3179
0.125	1.032	0.3319
0.125	1.056	0.3491
0.175	1.029	0.3242
0.175	1.045	0.3235
0.175	1.365	0.3447
0.250	1.332	0.3126
0.250	1.761	0.3183
0.450	2.275	0.2104

